Desalination and Water Treatment
www.deswater.com

doi: 10.5004/dwt.2022.27986

245 (2022) 226–237
January

Implementing eggplant peels as an efficient bio-adsorbent for treatment of oily domestic wastewater

Hyman J. Al-Jaaf[a], Nisreen S. Ali[a], Saja M. Alardhi[b], Talib M. Albayati[c,*]

[a]*College of Engineering, Department of Materials Engineering, University of Mustansiriyah, Baghdad, Iraq, emails: hymanjaaf@uomustansiriyah.edu.iq (H.J. Al-Jaaf), nisreensabah@uomustansiriyah.edu.iq (N.S. Ali)*
[b]*Nanotechnology and Advanced Materials Research Center, University of Technology – Iraq, 52 Alsinaa St., P.O. Box: 35010, Baghdad, Iraq, email: 11659@uotechnology.edu.iq*
[c]*Department of Chemical Engineering, University of Technology – Iraq, 52 Alsinaa St., P.O. Box: 35010, Baghdad, Iraq, email: Talib.M.Naieff@uotechnology.edu.iq*

Received 4 July 2021; Accepted 11 November 2021

ABSTRACT

The removal of oil from domestic wastewater was achieved by implementing eggplant peels (EPP) powder as an efficient bio-adsorbent material. The batch adsorption process was adopted to reach the acceptable range that allowed in Iraqi standardizations, which should not exceed (10 mg L^{-1}). The characterization of EPP was conducted with X-ray diffraction (XRD) spectroscopy, scanning electron microscopy (SEM), Fourier transform infrared (FT-IF) spectroscopy, and Brunauer–Emmett–Teller (BET). Two variables were taken into consideration, including time and temperature. It was noticed that these two variables had an essential impact in decreasing oil concentration in domestic wastewater. The temperature has an excellent effect comparing with time in decreasing the oil concentration from domestic wastewater; as both time and temperature increased, the oil concentration decreased. Results manifested that the adsorption method was effective in decreasing the oil concentration. Also, the results elucidated that the adsorption isotherms can be reasonably befitting via the Langmuir model due to the chemisorption that occurs on the surface between bio-adsorbent and pollutant with a determination coefficient of (0.8376). The adsorption kinetics of the oily west water upon the adsorbate was vigorously denoted via a pseudo-first-order kinetic model. The thermodynamic variables were assessed for determining free energy change ($\Delta G°$), enthalpy change ($\Delta H°$), and entropy change ($\Delta S°$).

Keywords: Wastewater treatment; Bio-adsorbent; Oily domestic wastewater; Eggplant peels; Adsorption process; Environmental pollution; Low cost adsorbent; Batch adsorption; Environment technology; Natural adsorbent

1. Introduction

The pollution of water is a highly significant problem which rises continuously as well as impends the living organism's sustainability because of the industrialization development and the rise in the population [1]. The oily wastewater pollution is chiefly revealed in the following features: imperiling human health; imperiling aquatic resources; atmospheric pollution; destructing the ordinary landscape; influencing crop manufacture, and influencing drinking water and groundwater resources [2]. Different modes of oily wastewater removal being evolved for limiting their impact in the environment such as; comprising coagulation [3,4], flotation [5], coagulation-flocculation [6], electrocoagulation [7,8], biological treatment [9,10], membrane separation technology [11], and adsorption [12–14]. These methods being obtainable for purifying the water, but the bio-adsorption method has attracted interest

* Corresponding author.

owing to its efficiency and ecologically kind nature. In the bio-adsorption methods, the agro-wastes may be the prospective origins to produce the bio-adsorbents, which can be utilized to improve the wastewater quality. In addition, it is inexpensive, freely obtainable, and easy to utilize [15]. Nevertheless, the adsorption is preferred via the manufacturing procedures owing to its realism and the simplicity of design, low price, the insensitivity to poisonous substances, the efficiency of processing, and the viability at too low concentrations [16–18]. The utilized adsorbents for the remediation of water being either of an ordinary origin or the results of industrial manufacture and/or the method of activation [19]. Eggplant is a normal vegetable that grows wholly everywhere in the world with a worldwide production ranked in the top six worldwide amount of (52.3) million tons in (2016) depended on FAO (Food and Agriculture Organization) reports [20,21]. Some studies used eggplant peel as an adsorbent, such as Ibrahim et al. [22] who practiced three ways of the eggplant peel activated charcoal (EPPAC) manufactured from the eggplant peel charcoal (EPPC). The factors that were used to produce the 3 activated charcoals, such as temperature and time were utilized in a new process. Gulistan et al. [23] observed that the efficiency of taking out the oil from the samples of created water (SPW) that is supplying a less-price adsorbent eggplant peel powder (EPP). Factors that were used to study the exclusion effectiveness are pH, time, and temperature. Yin et al. [24] measured the consequence of water presence over the hydrothermal performance process for the carbon aerogels (CAs) manufacture via utilizing the eggplant as a raw material.

In the present study, the most crucial aim of this work is that the eggplant peel powder as bio-adsorbent was manufactured from locally available material, that is reusable to reduce environmental pollution by implementing the low price and environmentally friendly bio-adsorbent material. Moreover, the adsorption mechanism and the isotherms of adsorption were investigated. Furthermore, real samples of oily wastewater have been treated using the eggplant peel powder beyond its characterization, and after that the influence of the various variables upon the treatment via adsorption process has been investigated, counting the contact time and temperature. The studies of isotherm, kinetics, and thermodynamic have been conducted for estimating the controlling mechanisms of the adsorption process.

2. Experimental

2.1. Materials and methods

Domestic real wastewater was taken from different areas in Baghdad city; the capital of Iraq, such as samples 1, 2, 3, and 4 of the eggplant peels powder. The oil content of the four real samples was measured before the adsorption process.

2.2. Characterization

The eggplant peels powder crystalline structure being characterized via XRD apparatus type (XRD-6000, Shimadzu, made in Japan), and the X-ray source releases radiation at a 0.15405 nm wavelength. This device operates at an emission current of 80 mA and 60 kV. The samples composition was specified via SEM device type (Tescan VEGA 3 SB, SEM). EPP chemical analysis was done using Fourier Transform Infrared (FT-IF) spectroscopy. The exact samples surface area was tested via BET instrument type (Q-surf 9600, made in the USA).

2.3. Adsorption experiments

The samples of wastewater were taken from different areas in Baghdad city; the capital of Iraq, such as; samples (1), (2), (3), and (4). To determine the optimal conditions for the oil adsorption process upon the powders of (EPP), samples of domestic wastewater being utilized are used. Solutions were made employing an entire volume of 50 mL for every solution that was being placed inside a 200 mL beaker, where 10 g of (EPP), as shown in Fig. 1, was then added to each beaker. These suspensions being then blended mixed for 10 min. 5 ml were taken from every suspension at definite intervals of time, after the end of each run, the sample was separated using a separator faunal (as depicted in Fig. 2) and was filtered for the residual oil concentration measurement. The oil concentration is obtained at a (225 nm) maximum wavelength via the UV-Vis spectrophotometer, type (U.V-1100, made in China). The adsorbed quantity for 1 g of EPP in mg g^{-1} or the capacity of adsorption (q), being performed utilizing this expression [25,26]:

$$q_e = \frac{\left(C_i - C_f\right)V}{M} \tag{1}$$

where q_e is capacity of adsorption at the adsorbent equilibrium (mg g^{-1}), C_i and C_f is initial and final concentrations (mg L^{-1}), V is the volume of solution in (L), M is adsorbents quantity (g). In addition, the removal percentage of oil (%R) being regarded as applying this expression [27,28]:

$$\%\text{Removal} = \frac{C_i - C_e}{C_i} \times 100 \tag{2}$$

where C_e in (mg L^{-1}) concentration of adsorbate at the equilibrium.

2.4. Isotherm model of adsorption

2.4.1. Isotherm of Langmuir

Such model presumes to create monolayer adsorption having an equivalent adsorption heat upon a surface. The formula of linearization is depicted as [29,30]:

$$\frac{C_e}{q_e} = \frac{C_e}{q_{\max}} + \frac{1}{b\, q_{\max}} \tag{3}$$

where $q_{\max}$ is the constant of Langmuir that associates to the capacity of adsorption (mg g^{-1}) and b represents a constant referring to the energy of adsorption (L mg^{-1}). Constants ($q_{\max}$) as well as (b) can be computed by Eq. (3) via the linear plot's slope of C_e/q_e vs. C_e. Furthermore, the dimensionless equilibrium factor (R_L) reveals that the isotherm being

Fig. 1. Eggplant peels powder.

Fig. 2. Separator faunal with treated sample.

"favourable", "irreversible", "linear", or "unfavourable" if the magnitude of R_L is <one, $R_L = 0$, $R_L = 1$, and $R_L >$ one, correspondingly. It is stated via Eq. (4) as [31,32]:

$$R_L = \frac{1}{1 + b\,C_i} \tag{4}$$

2.4.2. Isotherm of Freundlich

The surface energy depiction is completed utilizing the expression provided via [33]:

$$\ln q_e = \ln k_f + \frac{1}{n}\ln C_e \tag{5}$$

where k_f represents a constant that is associated with the capacity of sorbent adsorption; n represents the intensity of adsorption depended upon the n value, the "poor" adsorption, the "moderate" adsorption, and the "good" characteristics that obtained if the n value is <one, n is 1–2, and n = 2–10, correspondingly [20].

2.4.3. Isotherm of Temkin

The linearized formula of the model of the isotherm of Temkin being stated as [34]:

$$\ln q_e = \ln q_s + K_{\mathrm{DR}}^2 \tag{6}$$

where k_t is the binding constant in L g^{-1} at equilibrium corresponding to the ultimate energy of binding. $B = (RT/b)$ is the constant of Temkin in J kJ^{-1}. β is the adsorption heat in kJ mol^{-1}. R is the universal gas constant which is equal to 8.314 J mol^{-1} K^{-1}. T is the absolute temperature in K.

2.4.4. Dubinin–Radushkevich adsorption isotherm

The model is a semi-empirical equation in which adsorption follows a pore-filling mechanism. It presumes a multilayer character involving Van der Waal's forces, applicable for physical adsorption processes, and is a fundamental equation that qualitatively describes the adsorption of gases and vapors on microporous sorbents [35]. Dubinin–Radushkevich isotherm is expressed as follows:

$$\ln q_e = \ln q_s + K_{DR}\varepsilon^2 \tag{7}$$

$$\varepsilon = RT \ln\left(1 + \frac{1}{C_e}\right) \tag{8}$$

$$E = \frac{1}{\left(2K_{DR}\right)^{1/2}} \tag{9}$$

where q_s is the theoretical isotherm saturation capacity (mg g^{-1}), ε is Polanyi potential, K_{DR} is Dubinin–Radushkevich constant (mol $kJ)^{-2}$, and E is mean adsorption energy (kJ mol^{-1}).

2.5. Kinetics of adsorption

The adsorption rate constant being obtained via this first-order rate equation [36]:

$$\log\left(q_e - q_t\right) = \log q_e - \left(\frac{K_1}{2.303}t\right) \tag{10}$$

where q_t is the dye adsorbed amount at a time t (min). K_1 is the pseudo-first-order of the adsorption rate constant.

Expression of the pseudo-second-order equation being depended upon this formula:

$$\frac{t}{q_t} = \frac{1}{K_2 q_e^2} + \frac{1}{q_e}t \tag{11}$$

where K_2 is the pseudo-second-order of the adsorption rate constant in (g mg^{-1} min^{-1}), it can be evaluated via drawing t/q_t vs. t.

2.5.1. Intraparticle diffusion model

The possibility of film or intraparticle diffusion was explored by using the Weber–Morris model [37]:

$$q_t = K_p t^{0.5} + I \tag{12}$$

where K_p (mg g^{-1} min$^{-0.5}$) is the constant of intraparticle diffusion rate and I is the constant of the intraparticle diffusion.

2.5.2. Boyd model

It was reported [21–24] that the Boyd equation can be applied to determine the rate-controlling step for an adsorbent and expressed as [38,39]:

$$F = 1 - \left(\frac{6}{\pi^2}\right) e^{-B_t} \tag{13}$$

where B_t is the function of F and F is the fraction of solute adsorbed at different times, t. The F value can be calculated using:

$$F = \frac{q_t}{q_e} \tag{14}$$

It is hard to estimate appropriate values of B_t with Eq. (13); B_t can be calculated using the integrated Fourier transform of Eqs. (15) and (16):

$$0 \le F \le 0.85: \quad B_t = 2\pi - \left(\frac{\pi^2}{3} F\right) - 2\pi\left(1 - \left(\frac{\pi}{3} F\right)\right)^{\frac{1}{2}} \tag{15}$$

$$0.86 \le F \le 1: \quad B_t = -0.4977 - \ln\left(1 - F\right) \tag{16}$$

2.6. Thermodynamics of adsorption

The thermodynamic variables being assessed for determining the free energy change ($\Delta G°$), the enthalpy change ($\Delta H°$), and the entropy change ($\Delta S°$) employing the subsequent: the change of Gibbs free energy [40]:

$$\Delta G° = -RT \ln K_C \tag{17}$$

The obvious adsorption equilibrium constant (K_C) being described as [41]:

$$K_C = \frac{q_e}{C_e} \tag{18}$$

In such a state, the activity has to be utilized in place of the concentration for obtaining the standard thermodynamic equilibrium constant (K_C) of the adsorption scheme.

$$\Delta G° = \Delta H° - T\Delta S° \tag{19}$$

$$\ln K_C = \frac{\Delta S°}{R} - \frac{\Delta H°}{RT} \tag{20}$$

where $\Delta H°$ and $\Delta S°$ in (J mol^{-1}) being caused from the slope as well as the intercept of Van't Hoff system of $\ln K_C$ against ($1/T$) Eq. (12) [42].

3. Results and discussion

3.1. Adsorbents (EPP) characterization

EPP crystalline structure, phase structure, and structural character are being scrutinized via X-ray diffraction kind (Shimadzu-6000, made in Japan). The X-ray diffractometer having a range of (2θ) (10°–90°), a rate of a scan of (2°/min), and Cu-kα (λ is 1.541) as a radiation source being used, as depicted in Fig. 3. The XRD was employed for describing further structural details on the (EPP). The resulted pattern of (XRD) revealed in Fig. 3 manifested that the (EPP) crystalline structure is more than the amorphous rations since the sharp and the intense (366) signals seemed at 22°, 23°, 64°, and 78°. Therefore, the resulted outcomes proposed the (EPP) crystalline nature.

The EPP morphology analysis was carried out utilizing the scanning electron microscopy device, as shown in Fig. 4. Closer scoping upon the EPP surface guarantees the homogenous shape existence and smooth surfaces having a diameter around (50 μm), alike outcomes were documented via [43].

Fig. 5 illustrates the (FTIR) spectrum of eggplant peels powder. To investigate the chemical functional sets which are responsible for the adsorption, the EPP adsorbent (FTIR) analysis was done. In this figure, the existence of the wide adsorption peak at (3,334.91 cm^{-1}) as well as the peak at (1,060.84 cm^{-1}) that being the characteristic of hydroxyl bonds that vibrate in the stretching and bending motions can validate the hydroxyl sets presence upon the adsorbent surface where it is overlapped to a certain level with the (C–H) zone. Furthermore, the concentrated absorption peaks existence at (1,733.03 cm^{-1}) as well as (1,622.56 cm^{-1}) that correspond to the carboxylic acids in addition to the carboxylate functional sets exhibits the (C=O) groups existence upon the eggplant peel surface [44]. Thus, the spectra of the Fourier transform infrared evince the chemical functional sets' existence; that means hydroxyl [45] as well as carboxyl groups [46]. The BET surface area, the volume

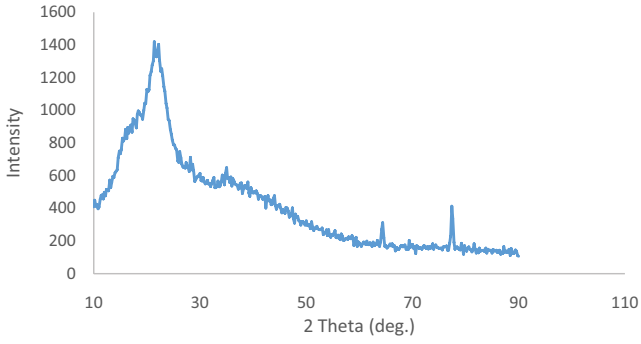

Fig. 3. XRD pattern of the eggplant peels powder bio-adsorbent.

of the pore, and the EPP sample's pore diameter being measured, and the summary of outcomes are given in Table 1. The values of oil concentration in water measured by UV device before adsorption at 20°C for four samples are shown in Fig. 6.

3.2. Experiments of batch adsorption

3.2.1. Contact time influence

Because the process of adsorption is a pollutant transfer from the liquid phase to a solid phase, the time of contact between these (2) phases possesses an influence upon the rate of mass transfer [47]. As a result, it's significant to investigate its influence upon the removal efficiency via eggplant peels powder as a bio-adsorbent. The resulted in outcomes via testing the contact time influence upon the performance of adsorption of oil concentration in water depending on eggplant peels powder as a bio-adsorbent are presented in Fig. 7 and supplementary material Tables S1–S4, which show the oil concentration before and after adsorption for four samples. The results showed that the oil concentration decreased by adsorption with increasing time until it is reached the concentration that does not exceed (10 mg L^{-1}) in real domestic wastewater.

The time of contact was obtained lengthier, the removal of oil also increased. That was owing to, at the start, the existence of effective sites in the EPP structure. Consequently, if the time of contact time is increased, then the effective sites upon the adsorbent are filled by the molecules of oil. However, by the rise of the time of contact, the sites of adsorptions initiate to decrease owing to that the molecules of oil begin filling the site of adsorption. That's if a second phase begins, the sluggish phase adsorption, where the adsorption still takes place but at sluggish adsorption [20,48].

Furthermore, it can be seen that the decrease in oil content was gradual, and over time the removal efficiency decreased as follows: Sample 3 > Sample 1 > Sample 2 > Sample 4, where the removal efficiency was equal to 75.6%,75.4%, 73.3%, 72.7%, the oil content in four samples after adsorption were approximately the same and referred to a good removal.

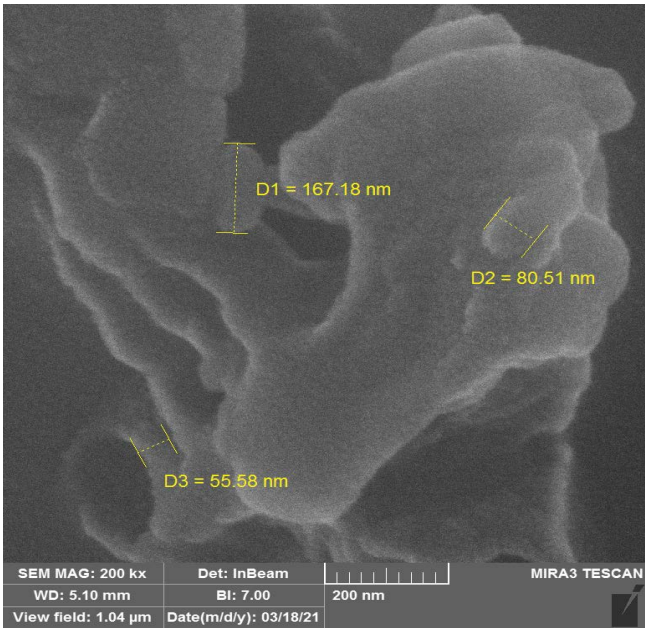

Fig. 4. Scanning electron microscopic (SEM) images of eggplant peels powder bio-adsorbent.

3.2.2. Influence of temperature

To discover the temperature influence level upon the oil concentration adsorption in water using eggplant peels powder as a bio-adsorbent material, the new work tested the temperature influence from (20°C–100°C) by increasing it (20°C) each time. It can be concluded from supplementary material Tables S5–S8 and Fig. 8 that the oil concentration decreased gradually with increasing the temperature.

Table 1
Structure properties of eggplant peels

Sample	S_{BET} (m^2 g^{-1})	V_p (cm^3 g^{-1})	*D*BJH (nm)
Eggplant peels	5.0766	0.015837	12.478

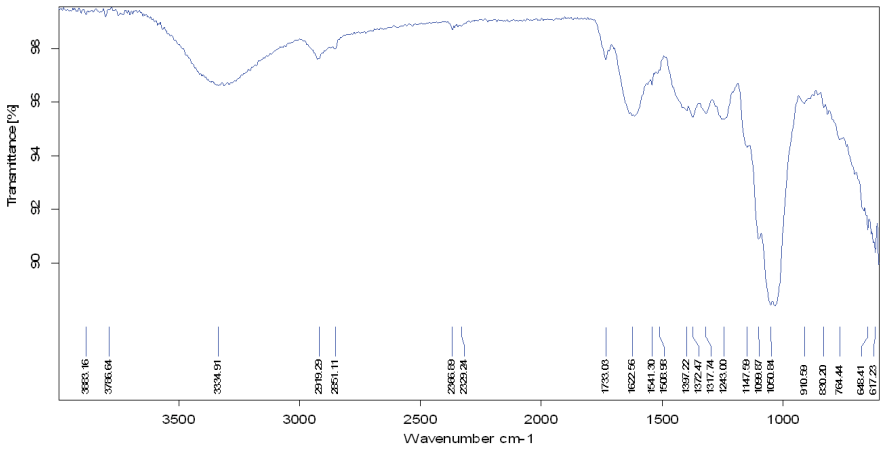

Fig. 5. FT-IR spectra of the eggplant peels powder bio-adsorbent.

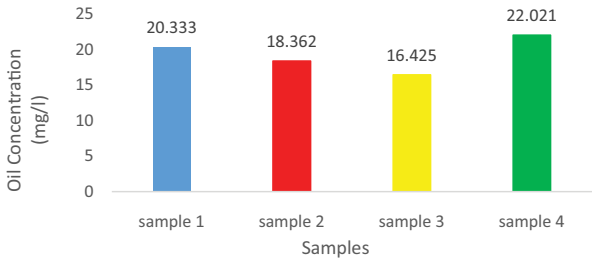

Fig. 6. Oil concentration for four samples before adsorption process.

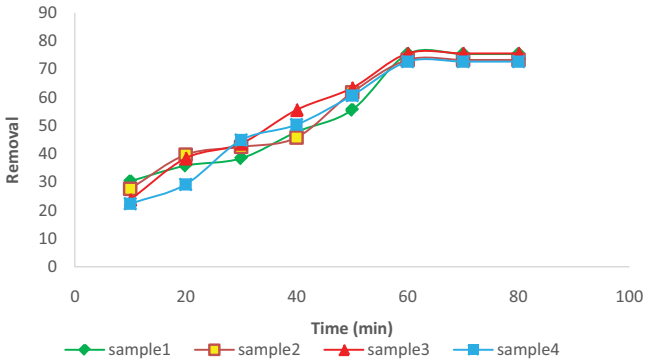

Fig. 7. Contact time influence upon the sample (1), sample (2), sample (3) and sample(4), oil removal (oil initial concentration = 20.333, 18.362, 16.425 and 22.021 mg L^{-1}, respectively, the dose of bio-adsorbent = 10 g, at temperature = 20°C).

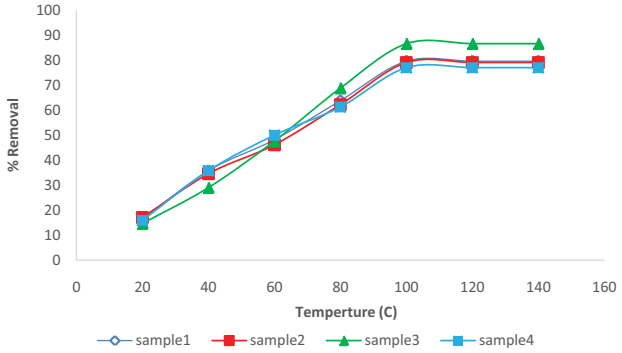

Fig. 8. Temperature influence upon sample (1), sample (2), sample (3) and sample (4), oil removal (oil initial concentration = 20.333, 18.362, 16.425 and 22.021 mg L^{-1}, the dose of bio-adsorbent = 10 g, at time of contact = 10 min).

The temperature is anticipated to be another vital parameter in the removal procedures of oil. To discover the temperature influence level upon the oil concentration adsorption in water using eggplant peels powder as an adsorbent material, the new work tested the influence of 20°C–100°C influence by increasing it 20°C each time. It can be concluded from supplementary material Tables S5–S7, and S8 that the oil concentration decreased gradually with increasing the temperature. The removal efficiency decreased as follows: Sample 3 > Sample 1 > Sample 2 > Sample 4, where the removal efficiency was equal to 86.7%, 79.7%, 79.1%, and 77.0%. The removal performance of oil begins to somewhat increase with more rise in the temperature. The viscosity of the oil is recognized to change in a reverse way with the temperature. As oil becomes thinner owing to the temperature rise, then, the molecules of oil begin diffusing into the pores inside the surface of EPP. The coefficient of mass transfer and the rate of diffusion begins to rise with a reduction in the viscosity [49,50]. This reduction in the viscosity would rise the oil molecules' free energy into samples; thus, these molecules have an increment in their arbitrary motion. The interaction between molecules of oil and surface sites of EPP gets further likely, resulting in the higher removal performance of the oil. The removal phenomenon of oil is enabled in an optimal range of temperature, whereas over a temperature of 100°C, the exothermic procedure is the governing variable for the adsorption.

3.3. Adsorption isotherms

They are significant for describing the way the adsorbates will interact with an adsorbent as well as being crucial in the optimization of the adsorbent usage [51]. The data of equilibrium adsorption were fitted into the isotherms of Langmuir, Freundlich, Temkin, and Dubinin–Radushkevich. For every isotherm, the equilibrium capacities, the rate constants, and the associated coefficients of correlation being elucidated in Fig. 9a–d. Being introduced in Table 2, the Langmuir isotherm gave the biggest coefficient of regression (R^2 = 0.837). This type of adsorption is considered to be a monolayer with equal distribution of heat to the surface [52]. The isotherms of Langmuir mean that there's no sturdy rivalry between the adsorbate and the solvent for occupying the adsorbent sites. Within such a state, the adsorbed molecules' longitudinal axes being parallel to the surface of the adsorbent [51]. The maximum adsorption capacity value, determined from the Langmuir model, is equal to 0.197 mg g^{-1}. The exponent (n) value offers a sign of the favorability of adsorption [53]. The studied material eggplant peels powder has moderate adsorption for oil, where n is equal to 1.567.

Table 2
The isotherm models' parameters

Langmuir			Freundlich			Temkin			Dubinin–Radushkevich			
q_{max} (mg g^{-1})	R_L	R^2	k_f (mg g^{-1})	n	R^2	β (kJ mol^{-1})	k_t (L g^{-1})	R^2	K_{DR} (mol kJ)$^{-2}$	E (kJ mol^{-1})	q_s (mg g^{-1})	R^2
0.197	0.284	0.837	0.025	1.567	0.828	0.0451	0.991	0.824	1.659	1.821	0.1	0.828

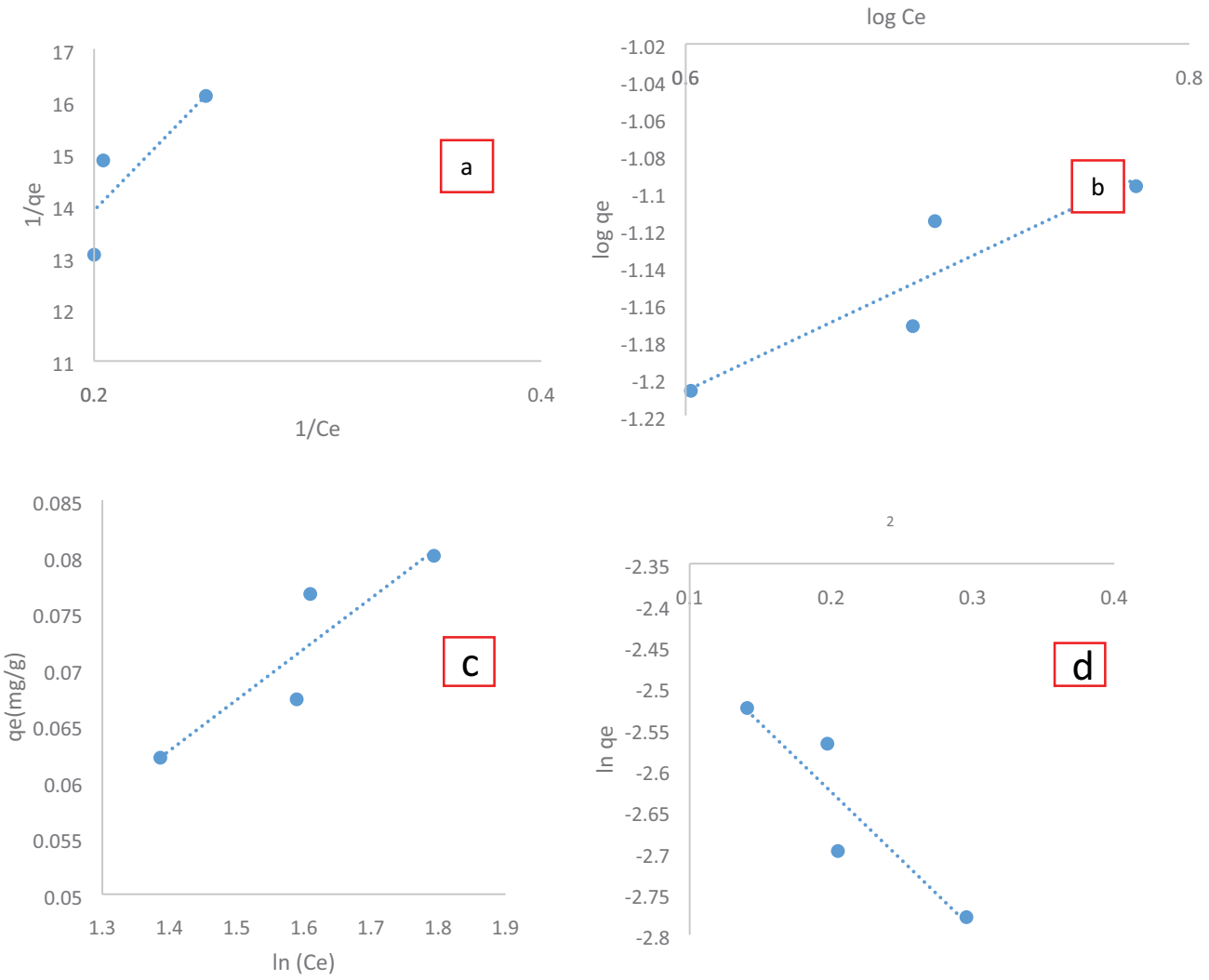

Fig. 9. The adsorption models of (a) Langmuir model, (b) Freundlich, (c) Temkin and (d) Dubinin–Radushkevich isotherms.

3.4. Adsorption kinetics models

Table 3, as well as Fig. 10a–d, denote the kinetic variables of the 3 suggested kinetic models. The correlation coefficient 0.925 of the 1st-order kinetic model being relatively greater than that obtained 0.717 from the second-order kinetic model, so the oil adsorption on EPP was suitable for a first-order reaction. The driving force for pseudo-first-order is stated as the discrepancy between the loading at a time and the last equilibrium loading (which is fixed for a specified first concentration and an adsorbent dose) [54]. The adsorption was suggested to be a diffusion process involving microspores [55].

3.5. Adsorption mechanism

Four main mechanisms describe the transfer of a solute from a solution to the adsorbent. The first is called mass transfer (bulk movement) of solute particles as soon as the adsorbent is dropped into the solution. This process is too fast, thus it is not considered during the design of kinetic systems. The second mechanism is called film diffusion; it involves the slow movement of solutes from the boundary layer to the adsorbent's surface. When the solute reaches the surface of the adsorbent, they move to the pores of the adsorbent—third mechanism. The final mechanism involves rapid adsorptive attachment of the solute on the active sites of the pores; being a rapid process, it is not considered during the engineering design of kinetics. If the system is characterized by poor mixing, small solute size, and low concentration, film diffusion becomes the rate-controlling step; otherwise, intraparticle diffusion (IP) controls the process. When the solute concentration is low, PSO explains the adsorption mechanism more than any other kinetic model; however, at high initial concentration, the PFO model is favored. This is because at low C_0 the value of $\ln(q_e - qt)$ increases exponentially increasing the error function—which is the reverse for high C_0 [56,57].

3.6. Adsorption thermodynamics parameters

The experimental outcomes of thermodynamic variables are listed in Table 4. The ($\Delta H°$) positive magnitude guarantees that adsorption is an endothermic reaction. Thus,

Table 3
Kinetic models

Pseudo-first-order			Pseudo-second-order			Intraparticle diffusion			Boyd model
q_e (mg g^{-1})	K_1 (min^{-1})	R^2	q_e (mg g^{-1})	K_2 (g mg^{-1} min^{-1})	R^2	I	K_p (mg g^{-1} min$^{-0.5}$)	R^2	R^2
0.060	0.0003	0.925	0.104	0.259	0.717	0.0036	0.009	0.839	0.899

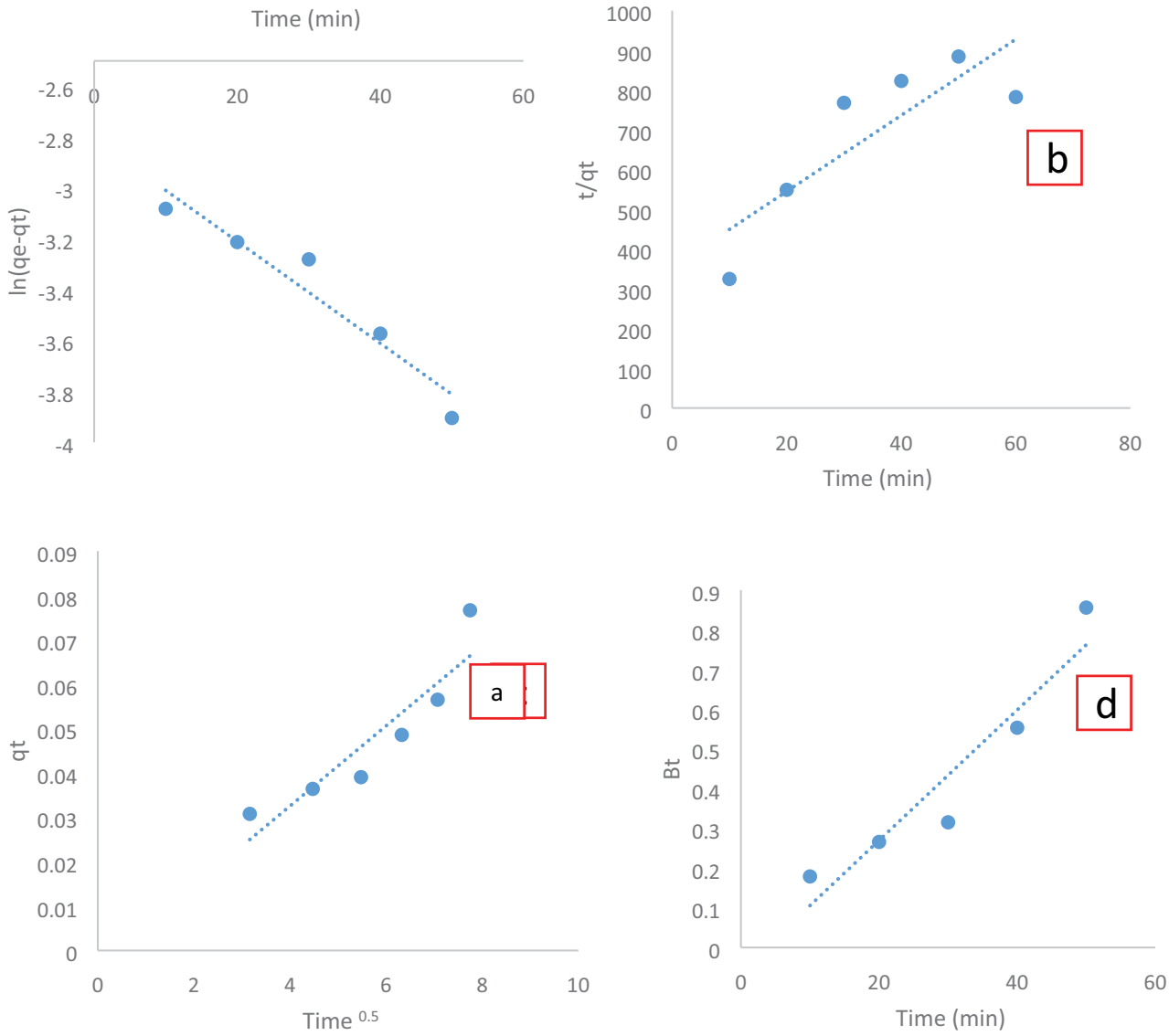

Fig. 10. Models of the (a) pseudo-first-order (b) pseudo-second-order (c) intraparticle diffusion and (d) Boyd kinetic for the process of adsorption.

the physical sorption being characterized via a small variation in enthalpy, distinctively from –10 to –40 kJ mol^{-1} (the sorption heats are within a 10–40 kJ mol^{-1} range), while the chemisorption heat being hardly <80 kJ mol^{-1} and frequently surpasses 400 kJ mol^{-1}. The $\Delta G°$ should continuously be positive for a technique has to be thermodynamically satisfactory [58]. The $\Delta G°$ negative magnitudes being the indications of the non-spontaneous nature of the sorption regime. The $\Delta S°$ positive magnitude confirms the arbitrariness rising at the adsorbate-solution interface through the process of adsorption.

4. Conclusions

The present research tested the adsorption of the oily domestic actual wastewater on the eggplant peels powder

Table 4
Thermodynamic variables for the process of adsorption

Temp. °K	$\Delta H°$ (kJ mol^{-1})	$\Delta G°$ (J mol^{-1})	$\Delta S°$ (J mol^{-1} K^{-1})
293		16,876	
313		15,302	
333	32,501.92	14,864	53.696
353		13,874	
373		12,186	

as an effective bio-adsorbent. Adsorption of the oily domestic real wastewater was obtained to be reliant upon the time of contact and the temperature. The isotherms of Langmuir, Freundlich, Temkin, and Dubinin–Radushkevich could wholly be employed for modeling the isothermal adsorption process in this investigation. The isotherm of Langmuir being the best fit adsorption isotherm compared to the isotherms of Freundlich as well as the Temkin and Dubinin–Radushkevich. Two kinetic models are being employed to model the adsorption mechanism of the oily domestic real wastewater on EPP. It was obtained that the adsorption kinetics fitted the pseudo-first-order kinetic better than other kinetic models as observed from the greater coefficient of correlation. The removal percentage rose by increasing the time of contact and the temperature, where the oil concentration was reduced gradually by rising the time for the real four samples. Furthermore, the concentration of oil after adsorption for four real samples was decreased gradually with increasing the temperature. It was concluded that the eggplant peels powder, a by-product from agricultural waste, can be efficiently employed as an efficient bio-adsorbent for eliminating the oily domestic actual wastewater.

Acknowledgment

The researchers thankfully acknowledge the support from the University of Mustansiriyah. This work is supported by the Chemistry Lab of the College of the Engineering/ University of Mustansiriyah-Baghdad-Iraq.

References

[1] C.M. Hussain, Handbook of Nanomaterials for Industrial Applications, Elsevier, 2018. Available at: https://doi.org/10.1016/C2016-0-04427-3
[2] L. Yu, M. Han, F. He, A review of treating oily wastewater, Arabian J. Chem., 10 (2017) S1913–S1922.
[3] C. Li-na, L. Yan-juan, H. Bin, Synthesis and application of PAZSC in oily wastewater treatment, Chem. Eng., 1 (2011) 5–9.
[4] E.K. Tetteh, S. Rathilal, Evaluation of different polymeric coagulants for the treatment of oil refinery wastewater, Cogent Eng., 7 (2020) 1–15.
[5] M.L. Hami, M.A. Al-Hashimi, M.M. Al-Doori, Effect of activated carbon on BOD and COD removal in a dissolved air flotation unit treating refinery wastewater, Desalination, 216 (2007) 116–122.
[6] G. Veréba, L. Nagya, S. Kertésza, I. Kovácsa, C. Hodúra, Z. László, Highly efficient purification of finely dispersed oil contaminated waters by coagulation/flocculation method and effects on membrane filtration, Studia UBB Chemia, 62 (2017) 259–270.
[7] F.Y. Al Jaberi, S.M. Jabbar, N.M. Jabbar, Modeling of adsorption isotherms of oil content through the electrocoagulation treatment of real oily wastewater, AIP Conf. Proc., 2213 (2020) 020041, doi: 10.1063/5.0000157.
[8] F.Y. AlJaberi, S.A. Ahmed, H.F. Makki, Electrocoagulation treatment of high saline oily wastewater: evaluation and optimization, Heliyon, 6 (2020) e03988.
[9] Q. Cai, Z. Zhu, B. Chen, B. Zhang, Oil-in-water emulsion breaking marine bacteria for demulsifying oily wastewater, Water Res., 149 (2019) 292–301.
[10] L. Guo Hua, Y. Zheng Fang, T. Kun, Z. YiHe, Biotreatment of heavy oil wastewater by combined up flow anaerobic sludge blanket and immobilized biological aerated filter in a pilot-scale test, Biochem. Eng. J., 72 (2013) 48–53.
[11] E.O. Ezugbe, S. Rathilal, Membrane technologies in wastewater treatment: a review, Membranes, 10 (2020) 89, doi: 10.3390/membranes10050089.
[12] S.M. Alardhi, F.Y. Al Jaberi, L.M. Al Saedi, Studying the treatability of different types of nanoparticles for oil content removal from oily wastewater produced from refinery process, Egypt. J. Chem., 63 (2020) 4963–4973.
[13] Y. Wang, Y. Zhou, L. Cai, J. Guo, Y. Xu, H. Zhang, L. Ji, W. Song, Facile preparation of charcoal nanomaterial from fishery waste with remarkable adsorption ability, Materials, 12 (2019) 1318, doi: 10.3390/ma12081318.
[14] M. Sulyman, M. Sienkiewicz, J. Haponiuk, S. Zalewski, New approach for adsorptive removal of oil in wastewater using textile fibers as alternative adsorbent, Acta Sci. Agric., 2 (2018) 1–6.
[15] S. Singhal, S. Agarwal, K. Bahukhandi, R. Sharma, N. Singhal, Bioadsorbent: a cost-effective method for effluent treatment, Int. J. Environ. Sci., 3 (2014) 151–156.
[16] S.M. Alardhi, T.M. Albayati, J.M. Alrubaye, A hybrid adsorption membrane process for removal of dye from synthetic and actual wastewater, Chem. Eng. Process., 6 (2020) 108–113.
[17] E. Asma, B. Fawzi, Removal of oil from water by calcium alginate hydrogel modified with maleic anhydride, J. Polym. Environ., 26 (2018) 2901–2916.
[18] M.A. Frezzini, A. Giuliano, J. Treacy, S. Canepari, L. Massimi, Food waste materials appear efficient and low-cost adsorbents for the removal of organic and inorganic pollutants from wastewater, Res. Dev. Mater. Sci., 5 (2018) 298–309.
[19] S.M. Alardhi, J.M. Alrubaye, T.M. Albayati, Adsorption of Methyl Green dye onto MCM-41: equilibrium, kinetics and thermodynamic studies, Desal. Water Treat., 179 (2020) 323–331.
[20] M. Kazemi, F. Khodaiyan, S.S. Hosseini, Utilization of food processing wastes of eggplant as a high potential pectin source and characterization of extracted pectin, Food Chem., 294 (2019) 339–346.
[21] M. Kazemi, F. Khodaiyan, S.S. Hosseini, Eggplant peel as a high potential source of high methylated pectin: ultrasonic extraction optimization and characterization, LWT, 105 (2019) 182–189.
[22] J.J. Rochín-Medina, J.A. Sotelo-Castroa, N.Y. Salazar-Salasc, J.A. López-Valenzuelac, K. Ramírez, Antioxidant and anti-Salmonella activities of eggplant peel compounds obtained by solvent-free calcium-based extraction, CyTA-J. Food, 17 (2019) 873–881.
[23] T.H. Ibrahim, Z.B. Babar, M.I. Khamis, Removal of lead(II) Ions from aqueous solution using eggplant peels activated charcoal, Sep. Sci. Technol., 50 (2015) 91–98.
[24] A.S. Gulistan, T.H. Ibrahim, M.I. Khamis, Y. ElSayed, Application of eggplant peels powder for the removal of oil from produced water, Desal. Water Treat., 57 (2016) 15724–15732.
[25] A. Yin, F. Xu, X. Zhang, Fabrication of biomass-derived carbon aerogels with high adsorption of oils and organic solvents: effect of hydrothermal and post-pyrolysis processes, Materials, 9 (2016) 758, doi: 10.3390/ma9090758.
[26] H. Ahmadi, M. Javanbakht, B. Akbari-Adergani, M. Shabanian, β-cyclodextrin based hydrophilic thin layer molecularly imprinted membrane with di(2-ethylhexyl) phthalate selective removal ability, J. Ind. Eng. Chem., 89 (2020) 416–427.
[27] T.M. Albayati, A.A. Sabri, D.B. Abed, Adsorption of binary and multi heavy metals ions from aqueous solution by amine

functionalized SBA-15 mesoporous adsorbent in a batch system, Desal. Water Treat., 151 (2019) 315–321.
[28] M. Mohammadi, M. Sedighi, M. Hemati, Removal of petroleum asphaltenes by improved activity of NiO nanoparticles supported on green AlPO-5 zeolite: process optimization and adsorption isotherm, Petroleum, 6 (2020) 182–188.
[29] K.R. Kalash, T.M. Albayati, Remediation of oil refinery wastewater implementing functionalized mesoporous materials MCM-41 in batch and continuous adsorption process, Desal. Water Treat., 220 (2021) 130–141.
[30] S.T. Kadhum, G.Y. Alkindi, T.M. Albayati, Eco friendly adsorbents for removal of phenol from aqueous solution employing nanoparticle zero-valent iron synthesized from modified green tea bio-waste and supported on silty clay, Chin. J. Chem. Eng., 36 (2020) 19–28.
[31] T.M. Albayati, A.M. Doyle, Shape-selective adsorption of substituted aniline pollutants from wastewater, Adsorpt. Sci. Technol., 31 (2013) 459–468.
[32] T.M. Albayati, I.K. Salih, H.F. Alazzawi, Synthesis and characterization of a modified surface of SBA-15 mesoporous silica for a chloramphenicol drug delivery system, Heliyon, 5 (2019) e02539.
[33] T.M. Albayati, A.A. Sabri, D.B. Abed, Functionalized SBA-15 by amine group for removal of Ni(II) heavy metal ion in the batch adsorption system, Desal. Water Treat., 174 (2020) 301–310.
[34] A.D. Salman, T. Juzsakova, R. Ákos, R.I. Ibrahim, M.A. Al-Mayyahi, S. Mohsen, T.A. Abdullah, E. Domokos, Synthesis and surface modification of magnetic Fe_3O_4@SiO_2 core-shell nanoparticles and its application in uptake of scandium(III) ions from aqueous media, Environ. Sci. Pollut. Res., 28 (2021) 28428–28443.
[35] N. Ayawei, A.N. Ebelegi, D. Wankasi, Modelling and interpretation of adsorption isotherms, J. Chem., 2017 (2017) 1–11.
[36] T.M. Albayati, A.A.A. Jassam, Synthesis and characterization of mesoporous materials as a carrier and release of prednisolone in drug delivery system, J. Drug Delivery Sci. Technol., 53 (2019) 101176, doi: 10.1016/j.jddst.2019.101176.
[37] W.J. Weber, J.C. Morris, Kinetics of adsorption on carbon from solution, J. Sanit. Eng. Div., 89 (1963) 31–60.
[38] W. Zhu, J. Liu, M. Li, Fundamental studies of novel zwitterionic hybrid membranes: kinetic model and mechanism insights into strontium removal, The Sci. World J., 2014 (2014) 1–7, doi: 10.1155/2014/485820.
[39] D. Reichenberg, Properties of ion-exchange resins in relation to their structure, III: kinetics of exchange, J. Am. Chem. Soc., 75 (1953) 589–597.
[40] Z. Huang, T. Wang, H. Yi, X. Li, Study on the adsorption of methylene blue from dye wastewater by Humulus Japonicus leaves, E3S Web Conf., 236 (2021) 03028, doi: 10.1051/e3sconf/202123603028.
[41] B. Belhamdi, Z. Merzougui, M. Trari, A. Addoun, A kinetic, equilibrium and thermodynamic study of L-phenylalanine adsorption using activated carbon based on agricultural waste (date stones), J. Appl. Res. Technol., 14 (2016) 354–366.
[42] A. Bouguettoucha, A. Reffas, D. Chebli, T. Mekhalif, A. Amrane, Novel activated carbon prepared from an agricultural waste, *Stipa tenacissima*, based on $ZnCl_2$ activation—characterization and application to the removal of methylene blue, Desal. Water Treat., 57 (2016) 24056–24069.
[43] M.H.K. Darvanjooghi, S.M. Davoodi, A.Y. Dursun, M.R. Ehsani, I. Karimpour, E. Ameri, Application of treated eggplant peel as a low-cost adsorbent for water treatment toward elimination of Pb^{2+}: kinetic modeling and isotherm study, Adsorpt. Sci. Technol., 36 (2018) 1112–1143.
[44] S.M. Davoodi, M. Sadeghi, M. Naghsha, A. Moheb, Olefin–paraffin separation performance of polyimide Matrimid®/silica nanocomposite membranes, RSC Adv., 6 (2016) 23746–23759.
[45] M.H.K. Darvanjooghi, M. Nasr Esfahany, Experimental investigation of the effect of nanoparticle size on thermal conductivity of in-situ prepared silica–ethanol nanofluid, Int. Commun. Heat Mass Transfer, 77 (2016) 148–154.
[46] V.K. Gupta, S. Agarwal, T.A. Saleh, Synthesis and characterization of alumina-coated carbon nanotubes and their application for lead removal, J. Hazard. Mater., 185 (2011) 17–23.
[47] S. Larous, A.-H. Meniai, The use of sawdust as by product adsorbent of organic pollutant from wastewater: adsorption of phenol, Energy Procedia, 18 (2012) 905–914.
[48] M. Sulyman, J. Namiesnik, A. Gierak, Low-cost adsorbents derived from agricultural by-products/wastes for enhancing contaminant uptakes from wastewater: a review, Pol. J. Environ. Stud., 26 (2017) 479–510.
[49] J. Li, M. Luo, C. Zhao, C. Li, W. Wang, Y. Zu, Y. Fu, Oil removal from water with yellow horn shell residues treated by ionic liquid, Bioresour. Technol., 128 (2013) 673–678.
[50] J. Febrianto, A.N. Kosasih, J. Sunarso, Y. Ju, N. Indraswati, S. Ismadji, Equilibrium and kinetic studies in adsorption of heavy metals using biosorbent: a summary of recent studies, J. Hazard. Mater., 162 (2009) 616–645.
[51] O. Hamdaoui, Batch study of liquid-phase adsorption of methylene blue using cedar sawdust and crushed brick, J. Hazard. Mater., 135 (2006) 264–273.
[52] K.Y. Foo, B.H. Hameed, Insights into the modeling of adsorption isotherm systems, Chem. Eng. J, 156 (2010) 2–10.
[53] R.E. Treybal, Mass Transfer Operations, McGraw-Hill, New York, 1980.
[54] E. Worch, Adsorption Technology in Water Treatment: Fundamentals, Processes, and Modeling, Walter de Gruyter, GmbH & Co. KG, Berlin, Germany, 2012, 345 p. Available at: https://doi.org/10.1515/9783110240238
[55] R.C. Bansal, M. Goyal, Activated Carbon Adsorption, 1st ed., CRC Press, 2005. Available at: https://doi.org/10.1201/9781420028812
[56] H.N. Tran, S. You, A.H. Bandegharaei, H. Chao, Mistakes and inconsistencies regarding adsorption of contaminants from aqueous solutions: a critical review, Water Res., 120 (2017) 88–116.
[57] S. Azizian, Kinetic models of sorption: a theoretical analysis, J. Colloid Interface Sci., 276 (2004) 47–52.
[58] U.J. Etim, S.A. Umoren, U.M. Eduok, Coconut coir dust as a low cost adsorbent for the removal of cationic dye from aqueous solution, J. Saudi Chem. Soc., 20 (2016) S67–S76.

Supplementary information

Table S1
Oil concentration before and after adsorption for sample 1

Run	Time (min)	Oil con. (mg L^{-1})
	Before adsorption	
1	0	20.333
	After adsorption	
1	0	17.032
2	10	14.176
3	20	13.05
4	30	12.522
5	40	10.616
6	50	9.03
7	60	5.0

Table S2
Oil concentration before and after adsorption for sample 2

Run	Time (min)	Oil con. (mg L^{-1})
	Before adsorption	
1	0	18.362
	After adsorption	
1	0	16.143
2	10	13.287
3	20	11.070
4	30	10.562
5	40	9.945
6	50	7.02
7	60	4.90

Table S3
Oil concentration before and after adsorption for sample 3

Run	Time (min)	Oil con. (mg L^{-1})
	Before adsorption	
1	0	16.425
	After adsorption	
1	0	14.362
2	10	12.525
3	20	10.105
4	30	9.243
5	40	7.287
6	50	6.012
7	60	4.0

Table S4
Oil concentration before and after adsorption for sample 4

Run	Time (min)	Oil con. (mg L^{-1})
	Before adsorption	
1	0	22.021
	After adsorption	
1	0	19.124
2	10	17.096
3	20	15.587
4	30	12.132
5	40	10.922
6	50	8.653
7	60	6.01

Table S5
Oil concentration before and after adsorption for sample 1

Run	Temp. (°C)	Oil con. (mg L^{-1})
	Before adsorption	
1	20	20.333
	After adsorption	
1	20	17.001
2	40	13.045
3	60	10.525
4	80	7.342
5	100	4.124

Table S6
Oil concentration before and after adsorption for sample 2

Run	Temp. (°C)	Oil con. (mg L^{-1})
	Before adsorption	
1	20	18.362
	After adsorption	
1	20	15.225
2	40	12.007
3	60	9.876
4	80	6.924
5	100	3.825

Table S7
Oil concentration before and after adsorption for sample 3

Run	Temp. (°C)	Oil con. (mg L^{-1})
Before adsorption		
1	20	16.425
After adsorption		
1	20	14.009
2	40	11.647
3	60	8.586
4	80	5.103
5	100	2.181

Table S8
Oil concentration before and after adsorption for sample 4

Run	Temp. (°C)	Oil con. (mg L^{-1})
Before adsorption		
1	20	22.021
After adsorption		
1	20	18.522
2	40	14.135
3	60	11.001
4	80	8.521
5	100	5.05